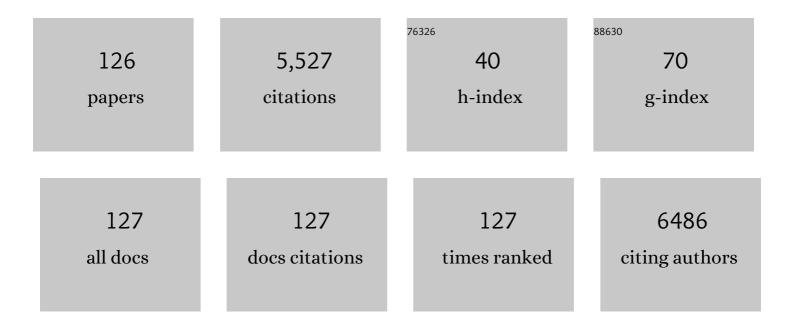
List of Publications by Year in descending order

Source: https://exaly.com/author-pdf/5229344/publications.pdf Version: 2024-02-01



#	Article	IF	CITATIONS
1	In-situ synthesis of direct solid-state Z-scheme V2O5/g-C3N4 heterojunctions with enhanced visible light efficiency in photocatalytic degradation of pollutants. Applied Catalysis B: Environmental, 2016, 180, 663-673.	20.2	620
2	Promoting visible-light-induced photocatalytic degradation of tetracycline by an efficient and stable beta-Bi2O3@g-C3N4 core/shell nanocomposite. Chemical Engineering Journal, 2018, 338, 137-146.	12.7	272
3	Synthesis, characterization and assembly of BiOCl nanostructure and their photocatalytic properties. CrystEngComm, 2009, 11, 1857.	2.6	210
4	Facile Synthesis and Assemblies of Flowerlike SnS <sub>2</sub> and In <sup>3+</sup> -Doped SnS <sub>2</sub> : Hierarchical Structures and Their Enhanced Photocatalytic Property. Journal of Physical Chemistry C, 2009, 113, 1280-1285.	3.1	201
5	Room temperature, template-free synthesis of BiOI hierarchical structures: Visible-light photocatalytic and electrochemical hydrogen storage properties. Dalton Transactions, 2010, 39, 3273.	3.3	169
6	Magnetic functional heterojunction reactors with 3D specific recognition for selective photocatalysis and synergistic photodegradation in binary antibiotic solutions. Journal of Materials Chemistry A, 2019, 7, 13986-14000.	10.3	140
7	In-situ synthesis and enhanced photocatalytic activity of visible-light-driven plasmonic Ag/AgCl/NaTaO3 nanocubes photocatalysts. Applied Catalysis B: Environmental, 2016, 191, 228-234.	20.2	126
8	In-situ approach to fabricate BiOI photocathode with oxygen vacancies: Understanding the N2 reduced behavior in photoelectrochemical system. Chemical Engineering Journal, 2019, 362, 349-356.	12.7	121
9	Efficient Electrocatalytic Oxidation of 5-Hydroxymethylfurfural Coupled with 4-Nitrophenol Hydrogenation in a Water System. ACS Catalysis, 2022, 12, 1545-1557.	11.2	113
10	Fabrication of TiO2/RGO/Cu2O heterostructure for photoelectrochemical hydrogen production. Applied Catalysis B: Environmental, 2016, 181, 7-15.	20.2	109
11	Solvothermal synthesis and electrochemical performance in super-capacitors of Co3O4/C flower-like nanostructures. Journal of Power Sources, 2014, 248, 1281-1289.	7.8	105
12	In-situ implantation of plasmonic Ag into metal-organic frameworks for constructing efficient Ag/NH2-MIL-125/TiO2 photoanode. Chemical Engineering Journal, 2020, 388, 124206.	12.7	98
13	An in situ photoelectroreduction approach to fabricate Bi/BiOCl heterostructure photocathodes: understanding the role of Bi metal for solar water splitting. Journal of Materials Chemistry A, 2017, 5, 4894-4903.	10.3	96
14	Organic Additives-Free Hydrothermal Synthesis and Visible-Light-Driven Photodegradation of Tetracycline of WO <sub>3</sub> Nanosheets. Industrial & Engineering Chemistry Research, 2014, 53, 5443-5450.	3.7	86
15	In-situ anchoring Ag through organic polymer for configuring efficient plasmonic BiVO4 photoanode. Chemical Engineering Journal, 2019, 358, 658-665.	12.7	81
16	Novel Multifunctional Nanocomposites: Magnetic Mesoporous Silica Nanospheres Covalently Bonded with Near-Infrared Luminescent Lanthanide Complexes. Langmuir, 2010, 26, 3596-3600.	3.5	78
17	MOF-derived Co3O4 thin film decorated BiVO4 for enhancement of photoelectrochemical water splitting. Applied Surface Science, 2019, 491, 497-504.	6.1	77
18	Synthesis of ternary spinel MCo2O4 (MÂ=ÂMn, Zn)/BiVO4 photoelectrodes for photolectrochemical water splitting. Chemical Engineering Journal, 2020, 392, 124838.	12.7	77

#	Article	IF	CITATIONS
19	Single-crystalline AgIn(MoO4)2 nanosheets grafted Ag/AgBr composites with enhanced plasmonic photocatalytic activity for degradation of tetracycline under visible light. Applied Catalysis B: Environmental, 2015, 164, 297-304.	20.2	74
20	Organic-inorganic hybrid-photoanode built from NiFe-MOF and TiO2 for efficient PEC water splitting. Electrochimica Acta, 2020, 349, 136383.	5.2	72
21	Ag-Decorated ATaO <sub>3</sub> (A = K, Na) Nanocube Plasmonic Photocatalysts with Enhanced Photocatalytic Water-Splitting Properties. Langmuir, 2015, 31, 9694-9699.	3.5	71
22	Synthesis and Optical Properties of Europium omplexâ€Doped Inorganic/Organic Hybrid Materials Built from Oxo–Hydroxo Organotin Nano Building Blocks. Chemistry - A European Journal, 2010, 16, 1903-1910.	3.3	67
23	Metal-organic framework derived Co3O4/TiO2 heterostructure nanoarrays for promote photoelectrochemical water splitting. International Journal of Hydrogen Energy, 2021, 46, 24965-24976.	7.1	67
24	Photorechargeable High Voltage Redox Battery Enabled by Ta <sub>3</sub> N <sub>5</sub> and GaN/Si Dualâ€Photoelectrode. Advanced Materials, 2017, 29, 1700312.	21.0	60
25	An <i>in situ</i> Bi-decorated BiOBr photocatalyst for synchronously treating multiple antibiotics in water. Nanoscale Advances, 2019, 1, 1124-1129.	4.6	60
26	Fabrication of MgFe <sub>2</sub> O <sub>4</sub> /MoS <sub>2</sub> Heterostructure Nanowires for Photoelectrochemical Catalysis. Langmuir, 2016, 32, 1629-1636.	3.5	59
27	Near-infrared luminescent xerogel materials covalently bonded with ternary lanthanide [Er(iii), Nd(iii), Yb(iii), Sm(iii)] complexes. Dalton Transactions, 2009, , 2406.	3.3	57
28	Controlled hydrothermal synthesis and magnetic properties of three-dimensional FeSe2 rod clusters and microspheres. Chemical Engineering Journal, 2013, 215-216, 508-516.	12.7	57
29	A study on the NIR-luminescence emitted from ternary lanthanide [Er(III), Nd(III) and Yb(III)] complexes containing fluorinated-ligand and 4,5-diazafluoren-9-one. Journal of Photochemistry and Photobiology A: Chemistry, 2010, 214, 152-160.	3.9	55
30	Semiconductors with NIR driven upconversion performance for photocatalysis and photoelectrochemical water splitting. CrystEngComm, 2014, 16, 3059.	2.6	54
31	Fabrication of TiO <sub>2</sub> –BiOCl double-layer nanostructure arrays for photoelectrochemical water splitting. CrystEngComm, 2014, 16, 820-825.	2.6	54
32	A study on the near-infrared luminescent properties of xerogel materials doped with dysprosium complexes. Dalton Transactions, 2009, , 6593.	3.3	53
33	Fabrication of BiVO4-Ni/Co3O4 photoanode for enhanced photoelectrochemical water splitting. Applied Surface Science, 2021, 538, 148150.	6.1	51
34	Understanding the key role of vanadium in p-type BiVO4 for photoelectrochemical N2 fixation. Chemical Engineering Journal, 2021, 414, 128773.	12.7	50
35	Photosensitive polymer and semiconductors bridged by Au plasmon for photoelectrochemical water splitting. Applied Catalysis B: Environmental, 2016, 195, 9-15.	20.2	49
36	Heterojunction composites of g-C3N4/KNbO3 enhanced photocatalytic properties for water splitting. International Journal of Hydrogen Energy, 2018, 43, 16566-16572.	7.1	46

#	Article	lF	CITATIONS
37	In situ constructing intramolecular ternary homojunction of carbon nitride for efficient photoinduced molecular oxygen activation and hydrogen evolution. Nano Energy, 2020, 75, 104865.	16.0	46
38	NIR-luminescence from ternary lanthanide [HoIII, PrIII and TmIII] complexes with 1-(2-naphthyl)-4,4,4-trifluoro-1,3-butanedionate. Journal of Luminescence, 2011, 131, 1857-1863.	3.1	45
39	Ex-situ flame co-doping of tin and tungsten ions in TiO2 nanorod arrays for synergistic promotion of solar water splitting. Chemical Engineering Science, 2020, 226, 115843.	3.8	44
40	InVO4 microspheres: Preparation, characterization and visible-light-driven photocatalytic activities. Chemical Engineering Journal, 2012, 200-202, 310-316.	12.7	43
41	ZIF-8 derived ZnO/TiO2 heterostructure with rich oxygen vacancies for promoting photoelectrochemical water splitting. Journal of Colloid and Interface Science, 2021, 603, 120-130.	9.4	42
42	Syngas production from methane steam reforming and dry reforming reactions over sintering-resistant Ni@SiO2 catalyst. Research on Chemical Intermediates, 2020, 46, 1735-1748.	2.7	37
43	Fabrication of Au@CdS/RGO/TiO <sub>2</sub> heterostructure for photoelectrochemical hydrogen production. New Journal of Chemistry, 2016, 40, 2287-2295.	2.8	36
44	Near-infrared luminescent copolymerized hybrid materials built from tin nanoclusters and PMMA. Nanoscale, 2010, 2, 2096.	5.6	35
45	Hydrothermal synthesis of porous rh-ln <sub>2</sub> O <sub>3</sub> nanostructures with visible-light-driven photocatalytic degradation of tetracycline. CrystEngComm, 2015, 17, 2336-2345.	2.6	35
46	Boosting Water Splitting Performance of BiVO <sub>4</sub> Photoanode through Selective Surface Decoration of Ag <sub>2</sub> S. ChemCatChem, 2018, 10, 4927-4933.	3.7	35
47	Amorphous MnCO <sub>3</sub> /C Double Layers Decorated on BiVO <sub>4</sub> Photoelectrodes to Boost Nitrogen Reduction. ACS Applied Materials & Interfaces, 2020, 12, 52763-52770.	8.0	35
48	Ag-Pi/BiVO4 heterojunction with efficient interface carrier transport for photoelectrochemical water splitting. Journal of Colloid and Interface Science, 2020, 579, 619-627.	9.4	35
49	Understanding the Z-scheme heterojunction of BiVO <sub>4</sub> /PANI for photoelectrochemical nitrogen reduction. Chemical Communications, 2021, 57, 10568-10571.	4.1	35
50	Biothiol-Functionalized Cuprous Oxide Sensor for Dual-Mode Sensitive Hg <sup>2+</sup> Detection. ACS Applied Materials & Interfaces, 2021, 13, 46980-46989.	8.0	34
51	Reasonable regulation of kinetics over BiVO4 photoanode by Fe–CoP catalysts for boosting photoelectrochemical water splitting. International Journal of Hydrogen Energy, 2019, 44, 28184-28193.	7.1	33
52	Charge-transfer dynamics at a Ag/Ni-MOF/Cu <sub>2</sub> O heterostructure in photoelectrochemical NH <sub>3</sub> production. Chemical Communications, 2021, 57, 8031-8034.	4.1	33
53	Enhanced photoelectrochemical water oxidation performance of a hematite photoanode by decorating with Au–Pt core–shell nanoparticles. Dalton Transactions, 2017, 46, 16050-16057.	3.3	32
54	Flame Reduced TiO <sub>2</sub> Nanorod Arrays with Ag Nanoparticle Decoration for Efficient Solar Water Splitting. Industrial & Engineering Chemistry Research, 2019, 58, 4818-4827.	3.7	32

#	Article	IF	CITATIONS
55	The synthesis of a novel Ag–NaTaO3 hybrid with plasmonic photocatalytic activity under visible-light. CrystEngComm, 2014, 16, 1384.	2.6	31
56	In-situ decoration of unsaturated Cu sites on Cu2O photocathode for boosting nitrogen reduction reaction. Chemical Engineering Journal, 2021, 413, 127453.	12.7	31
57	Near-infrared luminescent mesoporous MCM-41 materials covalently bonded with ternary thulium complexes. Microporous and Mesoporous Materials, 2009, 117, 278-284.	4.4	29
58	Integrated Heterostructure of PDA/Biâ€AgIn <sub>5</sub> S <sub>8</sub> /TiO <sub>2</sub> for Photoelectrochemical Hydrogen Production: Understanding the Synergistic Effect of Multilayer Structure. Advanced Materials Interfaces, 2018, 5, 1701574.	3.7	29
59	Dip-coating synthesis of P-doped BiVO4 photoanodes with enhanced photoelectrochemical performance. Journal of the Taiwan Institute of Chemical Engineers, 2018, 93, 582-589.	5.3	29
60	Fabrication of Zn-MOF decorated BiVO4 photoanode for water splitting. Colloids and Surfaces A: Physicochemical and Engineering Aspects, 2022, 640, 128412.	4.7	29
61	Microwave-assisted synthesis of hydrophilic BaYF <sub>5</sub> :Tb/Ce,Tb green fluorescent colloid nanocrystals. Dalton Transactions, 2011, 40, 142-145.	3.3	28
62	Silver nanoparticle toxicity in silkworms: Omics technologies for a mechanistic understanding. Ecotoxicology and Environmental Safety, 2019, 172, 388-395.	6.0	28
63	Efficient photoelectrochemical water oxidation of cobalt phthalocyanine decorated BiVO4 photoanode by improving kinetics. Applied Surface Science, 2021, 564, 150463.	6.1	27
64	Photoelectrochemical detection of 4-nitrophenol by sensitive Ni/Cu2O photocathode. Electrochimica Acta, 2021, 367, 137453.	5.2	26
65	Rod-in-tube nanostructure of MgFe <sub>2</sub> O <sub>4</sub> : electrospinning synthesis and photocatalytic activities of tetracycline. New Journal of Chemistry, 2016, 40, 538-544.	2.8	25
66	Near-infrared photoluminescent flowerlike α-In2Se3 nanostructures from a solvothermal treatment. Chemical Engineering Journal, 2013, 225, 474-480.	12.7	24
67	Hydrothermal synthesis of <font>Fe</font> <sub>2</sub> <font>O</font> <sub>3</sub> / <font>ZnO</font> heterojunction photoanode for photoelectrochemical water splitting. Functional Materials Letters, 2015, 08, 1550058.	1.2	24
68	A facile one-step solvothermal synthesis of bismuth phosphate–graphene nanocomposites with enhanced photocatalytic activity. Journal of Colloid and Interface Science, 2014, 435, 156-163.	9.4	23
69	Synthesis, characterization, and near-infrared luminescent properties of the ternary thulium complex covalently bonded to mesoporous MCM-41. Journal of Solid State Chemistry, 2009, 182, 435-441.	2.9	22
70	Self-Assembled Growth of AgIn(MoO4)2 Submicroplates into Hierarchical Structures and Their Near-Infrared Luminescent Properties. Crystal Growth and Design, 2009, 9, 848-852.	3.0	22
71	Dual-functional electrochemical bio-sensor built from Cu2O for sensitively detecting the thiols and Hg2+. Applied Surface Science, 2021, 564, 150397.	6.1	22
72	A new inorganic–organic hybrid In2Se3(en) as hollow nanospheres: hydrothermal synthesis and near-infrared photoluminescence properties. Dalton Transactions, 2013, 42, 2887.	3.3	21

#	Article	IF	CITATIONS
73	Effect of unsaturated coordination on photoelectrochemical properties of Ni-MOF/TiO2 photoanode for water splitting. International Journal of Hydrogen Energy, 2021, 46, 17741-17750.	7.1	21
74	Photoelectrochemical reduction of nitrate to ammonia over CuPc/CeO2 heterostructure: Understanding the synergistic effect between oxygen vacancies and Ce sites. Chemical Engineering Journal, 2022, 433, 133225.	12.7	21
75	In Situ Electrochemical Reconstitution of CF–CuO/CeO <sub>2</sub> for Efficient Active Species Generation. Inorganic Chemistry, 2022, 61, 8940-8954.	4.0	21
76	In Situ Decorating Coordinatively Unsaturated Fe Sites for Boosting Water Oxidation Performance of TiO 2 Photoanode. Energy Technology, 2019, 7, 1801128.	3.8	20
77	Boosted Photoelectrochemical N <sub>2</sub> Reduction over Mo <sub>2</sub> C In Situ Coated with Graphitized Carbon. Langmuir, 2020, 36, 14802-14810.	3.5	20
78	Synthesis, characterization and optical property of flower-like indium tin sulfide nanostructures. Dalton Transactions, 2009, , 1620.	3.3	19
79	Hydrothermal synthesis and thermoelectric transport properties of Sb2Te3–Te heterogeneous nanostructures. CrystEngComm, 2013, 15, 2978.	2.6	19
80	Sandwichâ€Nanostructured NiO–ZnO Nanowires@αâ€Fe <sub>2</sub> O <sub>3</sub> Film Photoanode with a Synergistic Effect and p–n Junction for Efficient Photoelectrochemical Water Splitting. ChemElectroChem, 2014, 1, 2089-2097.	3.4	19
81	Titanium dioxide macroporous materials doped with iron: synthesis and photo-catalytic properties. CrystEngComm, 2014, 16, 116-122.	2.6	19
82	Synthesis and luminescent properties of organic–inorganic hybrid macroporous materials doped with lanthanide (Eu/Tb) complexes. Optical Materials, 2011, 33, 582-585.	3.6	18
83	Luminescent character of mesoporous silica with Er2O3 composite materials. Microporous and Mesoporous Materials, 2013, 170, 113-122.	4.4	18
84	Facile Synthesis and Optical Property of Porous Tin Oxide and Europium-Doped Tin Oxide Nanorods through Thermal Decomposition of the Organotin. Journal of Physical Chemistry C, 2008, 112, 19939-19944.	3.1	16
85	Guests inducing p-sulfonatocalix[4]arenes into nanocapsule and layer structure. Journal of Solid State Chemistry, 2010, 183, 1457-1463.	2.9	15
86	Fabrication and characterization of magnetic mesoporous silica nanospheres covalently bonded with europium complex. Dalton Transactions, 2010, 39, 5166.	3.3	15
87	Electrospinning synthesis and photocatalytic property of CaFe <sub>2</sub> O <sub>4</sub> /MgFe <sub>2</sub> O <sub>4</sub> heterostructure for degradation of tetracycline. Crystal Research and Technology, 2015, 50, 244-249.	1.3	15
88	Culn(WO4)2 nanospindles and nanorods: controlled synthesis and host for lanthanide near-infrared luminescence properties. CrystEngComm, 2009, 11, 1987.	2.6	14
89	Novel Holmium (Ho) and Praseodymium (Pr) ternary complexes with fluorinated-ligand and 4,5-diazafluoren-9-one. Materials Letters, 2011, 65, 1642-1644.	2.6	14
90	Cubic spinel In4SnS8: electrical transport properties and electrochemical hydrogen storage properties. Dalton Transactions, 2010, 39, 7021.	3.3	13

#	Article	IF	CITATIONS
91	Erbium omplexâ€Doped Nearâ€Infrared Luminescent and Magnetic Macroporous Materials. European Journal of Inorganic Chemistry, 2008, 2008, 5513-5518.	2.0	12
92	Rare-Earth-Doped Bifunctional Alkaline-Earth Metal Fluoride Nanocrystals via a Facile Microwave-Assisted Process. Inorganic Chemistry, 2011, 50, 5327-5329.	4.0	12
93	Synthesis and Photoelectrochemical Properties of Efficient Photoanodes Built from Fe <sub>2</sub> O <sub>3</sub> /NiO Heterostructures. European Journal of Inorganic Chemistry, 2014, 2014, 3608-3613.	2.0	12
94	Electrospinning synthesis and photocatalytic property of Fe 2 O 3 /MgFe 2 O 4 heterostructure for photocatalytic degradation of tetracycline. Materials Letters, 2016, 176, 1-4.	2.6	12
95	Ni-MOF <i>in-situ</i> Decorating ZnO photoelectrode for photoelectrochemical water splitting. Functional Materials Letters, 2018, 11, 1850085.	1.2	12
96	Fabrication of an amorphous metal oxide/p-BiVO <sub>4</sub> photocathode: understanding the role of entropy for reducing nitrate to ammonia. Inorganic Chemistry Frontiers, 2022, 9, 805-813.	6.0	12
97	Inorganic salt-assisted hydrothermal synthesis and excellent visible light-driven photocatalytic performance of 3D MnNb <sub>2</sub> O <sub>6</sub> flower-like nanostructures. CrystEngComm, 2014, 16, 9255-9265.	2.6	11
98	Electrocatalytic reduction of 4-nitrophenol over Ni-MOF/NF: understanding the self-enrichment effect of H-bonds. Chemical Communications, 2022, 58, 4897-4900.	4.1	11
99	Controlled hydrothermal synthesis of three-dimensional FeSe2 rod clusters. Micro and Nano Letters, 2012, 7, 1076-1079.	1.3	10
100	Metal(II) coordination polymers based on a flexible N,N′,N″-tris(3-pyridyl)-1,3,5-benzenetricarboxamide ligand and organic polycarboxylate ligands: Syntheses, structures, and luminescence. Polyhedron, 2013, 50, 193-199.	2.2	10
101	In-situ synthesis of Co3O4/NaTaO3 composites by electrostatic attraction from Co-MOF for water splitting. Journal of Solid State Chemistry, 2019, 280, 120986.	2.9	10
102	Promoting photoelectrochemical hydrogen production performance by fabrication of Co1-XS decorating BiVO4 photoanode. International Journal of Hydrogen Energy, 2022, 47, 940-949.	7.1	10
103	An in-situ cation exchange approach to stabilize Zn-MOF: Understanding the role of nickel ions for photoelectrochemical performance. International Journal of Hydrogen Energy, 2022, 47, 10277-10288.	7.1	10
104	Confined growth of Co–Pi co-catalyst by organic semiconductor polymer for boosting the photoelectrochemical performance of BiVO <sub>4</sub> . New Journal of Chemistry, 2019, 43, 8160-8167.	2.8	9
105	An effective route for growth of WO3/BiVO4 heterojunction thin films with enhanced photoelectrochemical performance. Journal of Industrial and Engineering Chemistry, 2021, 104, 146-154.	5.8	9
106	Controllable TiO2 heterostructure with carbon hybrid materials for enhanced photoelectrochemical performance. New Journal of Chemistry, 2017, 41, 3460-3465.	2.8	8
107	One-step syntheses of MoS2/graphitic carbon composites with enhanced photocatalytic activity under visible light irradiation. New Journal of Chemistry, 2017, 41, 14171-14178.	2.8	8
108	A simple flame strategy for constructing Wâ€doped BiVO <sub>4</sub> photoanodes with enhanced photoelectrochemical water splitting. International Journal of Energy Research, 2020, 44, 10821-10831.	4.5	8

#	Article	IF	CITATIONS
109	Facile synthesis and optical properties of hybrid micro-wires based on Ln(DBM)3·H2O complexes. CrystEngComm, 2012, 14, 7287.	2.6	7
110	A novel binder-free electrode of graphene film upon intercalation of hollow MoS <sub>2</sub> spheres for enhanced supercapacitor performance. Functional Materials Letters, 2018, 11, 1850074.	1.2	7
111	Fabrication of ferric oxide/reduced graphene oxide/cadmium sulfide heterostructure photoelectrode for enhanced photoelectrochemical performance. Crystal Research and Technology, 2016, 51, 656-662.	1.3	6
112	Synthesis and photocatalytic property of porous metal oxides nanowires based on carbon nanofiber template. Functional Materials Letters, 2015, 08, 1550018.	1.2	5
113	Synthesis, structure and electrochemical behavior of a 3D crystalline copper(II) metal-organic framework. Functional Materials Letters, 2014, 07, 1450049.	1.2	4
114	Fabrication of stable photoanode built from ZnO nanosheets in situ decorated with carbon film. Functional Materials Letters, 2017, 10, 1750068.	1.2	4
115	Core-Shell Nanospheres (HP-Fe <sub>2</sub> O <sub>3</sub> @TiO <sub>2</sub> ) with Hierarchical Porous Structures and Photocatalytic Properties. Wuli Huaxue Xuebao/ Acta Physico - Chimica Sinica, 2013, 29, 167-175.	4.9	4
116	HYDROTHERMAL SYNTHESIS, CRYSTAL STRUCTURE AND ELECTROCHEMICAL BEHAVIOR OF 2D HYBRID COORDINATION POLYMER. Functional Materials Letters, 2013, 06, 1350027.	1.2	3
117	LUMINESCENT TITANIA MACROPOROUS MATERIALS DOPED WITH <font>Eu</font> ( <font>DBM</font> ) <sub>3</sub> â< <font>H</font> <sub>2</sub> <font>O</font> COMPLEX. Functional Materials Letters, 2013, 06, 1350060.	1.2	2
118	Synthesis, crystal structure and luminescent property of a zinc coordination polymer containing N,N′,N″â€ŧris(3â€pyridyl)â€1,3,5â€benzenetricarboxamide ligand. Crystal Research and Technology, 2014, 731-735.	49,3	2
119	Preparation of WO3 thin films by dip film-drawing for photoelectrochemical performance. Chinese Journal of Chemical Engineering, 2019, 27, 1207-1211.	3.5	2
120	The Facile Synthesis of SnSb/Graphene Composites and Their Enhanced Electrochemical Performance for Lithium-Ion Batteries. Science of Advanced Materials, 2013, 5, 1801-1806.	0.7	2
121	Fabrication and Photocatalytic Properties of MgFe2O4/rGO/V2O5 Heterostructure Nanowires. , 0, , .		2
122	Facile Preparation of Cu(OH) <sub>2</sub> @TiO <sub>2</sub> Nanowire Arrays for Photoelectrochemical Water Splitting. Advanced Materials Research, 0, 881-883, 968-971.	0.3	1
123	Synthesis, structures, and photoluminescence properties of three metal(II) coordination polymers derived from a flexible tripodal ligand and 2,6-pyridinedicarboxylic acid. Transition Metal Chemistry, 2013, 38, 157-163.	1.4	0
124	Design and Synthesis of Metal Oxides Doped Three-Dimensional Order Macroporous Materials Based on SiO <sub>2</sub> Matrixes and their Photocatalytic Property. Advanced Materials Research, 0, 807-809, 553-556.	0.3	0
125	Relationship between Planes of Cu <sub>2</sub> O Microcrystal and Photo-Catalytic Degradation of Methylene Blue. Advanced Materials Research, 0, 807-809, 562-566.	0.3	0
126	A green and low-cost approach for the large-scale production of uniform t-Se microspheres and their photoluminescence properties. Materials Letters, 2014, 116, 247-250.	2.6	0